Targeted Resequencing and Functional Testing Identifies Low-Frequency Missense Variants in the Gene Encoding GARP as Significant Contributors to Atopic Dermatitis Risk

Judith Manz[1,2,8], Elke Rodríguez[3,8], Abdou ElSharawy[4,5,8], Eva-Maria Oesau[6], Britt-Sabina Petersen[4], Hansjörg Baurecht[3], Gabriele Mayr[4], Susanne Weber[7], Jürgen Harder[3], Eva Reischl[1,2], Agatha Schwarz[3], Natalija Novak[6,8], Andre Franke[4,8] and Stephan Weidinger[3,8]

Gene-mapping studies have consistently identified a susceptibility locus for atopic dermatitis and other inflammatory diseases on chromosome band 11q13.5, with the strongest association observed for a common variant located in an intergenic region between the two annotated genes *C11orf30* and *LRRC32*. Using a targeted resequencing approach we identified low-frequency and rare missense mutations within the *LRRC32* gene encoding the protein GARP, a receptor on activated regulatory T cells that binds latent transforming growth factor-β. Subsequent association testing in more than 2,000 atopic dermatitis patients and 2,000 control subjects showed a significant excess of these *LRRC32* variants in individuals with atopic dermatitis. Structural protein modeling and bioinformatic analysis predicted a disruption of protein transport upon these variants, and overexpression assays in $CD4^+CD25^-$ T cells showed a significant reduction in surface expression of the mutated protein. Consistently, flow cytometric (FACS) analyses of different T-cell subtypes obtained from atopic dermatitis patients showed a significantly reduced surface expression of GARP and a reduced conversion of $CD4^+CD25^-$ T cells into regulatory T cells, along with lower expression of latency-associated protein upon stimulation in carriers of the *LRRC32* A407T variant. These results link inherited disturbances of transforming growth factor-β signaling with atopic dermatitis risk.

Journal of Investigative Dermatology (2016) ■, ■–■; doi:10.1016/j.jid.2016.07.009

INTRODUCTION

Atopic dermatitis (AD) is the most common chronic inflammatory skin condition. Although the pathomechanisms of AD are not fully understood, it is widely agreed that both abnormalities of the epidermal barrier function and a dysregulation of T-cell immunity with an imbalance of effector and regulatory T cell (Treg) responses lead to chronic inflammation, which extends beyond the skin and contributes to an increased risk for inflammatory comorbidities such as asthma, inflammatory bowel disease, and arthritis (Weidinger and Novak, 2016).

The immune abnormalities observed in AD and its common comorbidities are in part genetically predetermined, as evidenced by shared susceptibility genes that regulate T-cell differentiation and effector function or encode components of the innate immune system. Among such shared susceptibility regions is the chromosome band 11q13.5 locus, where variants located between the two annotated genes, *C11orf30* (coding for the protein EMSY) and *LRRC32* (coding for the protein GARP), have been associated with AD, asthma, Crohn's disease, ulcerative colitis, allergic sensitization, allergic rhinitis, eosinophilic esophagitis, and alopecia areata (Anderson et al., 2011; Barrett et al., 2008; Betz et al., 2015; Bonnelykke et al., 2013; Ellinghaus et al., 2013; Esparza-Gordillo et al., 2009; Ferreira et al., 2011; Franke et al.,

[1]*Research Unit of Molecular Epidemiology, Helmholtz Zentrum München, German Research Center for Environmental Health, Neuherberg, Germany;* [2]*Institute of Epidemiology II, Helmholtz Zentrum München, German Research Center for Environmental Health, Neuherberg, Germany;* [3]*Department of Dermatology, Venereology and Allergy, University Hospital Schleswig-Holstein, Campus Kiel, Kiel, Germany;* [4]*Institute of Clinical Molecular Biology, Christian-Albrechts-University of Kiel, Kiel, Germany;* [5]*Faculty of Sciences, Division of Biochemistry, Chemistry Department, Damietta University, New Damietta City, Egypt;* [6]*Department of Dermatology and Allergy, University Hospital Bonn, Bonn, Germany; and* [7]*Institute of Experimental Genetics, Genome Analysis Center, Helmholtz Zentrum München, German Research Center for Environmental Health, Neuherberg, Germany*

[8]*These authors contributed equally to this work.*

Correspondence: Stephan Weidinger, Department of Dermatology, Venereology and Allergy, University Hospital Schleswig-Holstein, Campus Kiel, Schittenhelmstrasse 7, 24105 Kiel, Germany. E-mail: sweidinger@dermatology.uni-kiel.de

Abbreviations: AD, atopic dermatitis; C11orf30, chromosome 11 open reading frame 30; GARP, glycoprotein A repetitions predominant; LAP, latency associated protein; LRRC32, leucine rich repeat containing 32; PBS, phosphate-buffered saline; SNV, single nucleotide variant; TGF-β, transforming growth factor-beta; Treg, regulatory T cell; WT, wild type

Received 22 January 2016; revised 14 June 2016; accepted 5 July 2016; accepted manuscript published online 21 July 2016; corrected proof published online XXX

© 2016 The Authors. Published by Elsevier, Inc. on behalf of the Society for Investigative Dermatology.

2010; Kottyan et al., 2014; Paternoster et al., 2012; Ramasamy et al., 2011; Weidinger et al., 2013). The causal gene and variants underlying this association signal, however, are yet unknown. Both genes located next to the associated markers encode proteins that represent promising biological candidates. EMSY has been reported to regulate nuclear receptor-mediated transcription (Garapaty et al., 2009) and interferon-stimulated gene expression (Ezell et al., 2012), and GARP encodes a surface receptor on activated Tregs that binds latent TGF-β (transforming growth factor-β) and modulates peripheral tolerance and T effector cell function (Tran et al., 2009; Wang et al., 2012). We set out to refine the 11q13.5 disease association signals using a combination of sequencing and functional annotation.

RESULTS AND DISCUSSION

Targeted next-generation sequencing of 11q13.5 (chromosome 11:75,800,000−76,070,000; NCBI36/hg18) in 31 AD patients selected from the original genome-wide association study (Esparza-Gordillo et al., 2009) and enriched for low-frequency-risk haplotypes and subsequent validation by Sanger sequencing identified two missense variants (A407T/rs79525962, R518W/rs142940671) in *LRRC32* with a minor allele frequency less than 0.01 in the 1000 Genomes Project (The International Genome Sample Resource, 2016) and/or without annotation in dbSNP 132 (National Center for Biotechnology Information, 2016). An extended mutational screening of the coding regions of *LRRC32* in 100 independent AD patients identified four additional rare missense single nucleotide variants (SNVs): R312C/rs371900727, S411R/rs201431152, R414W (without annotation in dbSNP 132), and R652C/rs143082901. No rare missense variants fulfilling our filter criteria were identified in *C11orf30*. All six *LRRC32* variants were carried forward to frequency assessment and association testing in an independent set of 2,193 German AD patients and 2,197 control subjects from the German population-based PopGen cohort (Krawczak et al., 2006) (see Supplementary Table S1 online). Cumulative minor allele tests showed a significant excess of rare alleles in AD ($P = 0.002$, allele carriers AD = 6.1% vs. allele carriers control subjects = 4.2%), and a suggestive significant association for allergic sensitization as an intermediate trait ($P = 0.02$). The most frequent variant, A407T/rs79525962, showed an odds ratio of 1.46 (95% confidence interval = 1.11−1.92, $P = 0.007$). A407T/rs79525962 is in complete linkage disequilibrium ($D' = 1$) with previously reported genome-wide association study risk SNPs for different inflammatory traits within the 11q locus (see Supplementary Table S2 online).

To predict the functional consequences of the identified variants, we performed structural protein modeling based on the toll-like receptor regulator CD180. The 21 leucine-rich repeats of the GARP extracellular domain likely fold into an alpha/beta horseshoe shape, in which leucine-rich beta-strands form a characteristic concave inner surface (see Supplementary Figure S1 online). GARP disulfide links with latent TGF-β, but noncovalent bonds are also sufficient for protein-protein interaction (Wang et al., 2012), and several N-glycosylation sites have been predicted or verified for GARP (Chen et al., 2009).

Analysis of *LRRC32*/GARP mRNA expression levels in different tissues and cell types, including skin, fibroblasts, keratinocytes, and peripheral blood mononuclear cells showed an ubiquitous expression with, however, variable levels (see Supplementary Figure S2 online).

All six identified SNVs lead to changes in the physicochemical properties of the affected amino acids and may consequently interfere with proper protein folding and function. The loss of positive charge on the protein surface as a consequence of arginine mutations (R312C, R414W, and R518W) may disturb potential protein interactions. Further, missense variants may cause local structural rearrangements near N-glycosylation sites that may hamper posttranslational modifications. Therefore, the identified *LRRC32* missense variants are not assumed to directly interfere with TGF-β binding but rather obstruct proper protein folding or hamper posttranslational modifications necessary for protein transport.

The most frequent variant, A407T/rs79525962, was subjected to further functional studies. *LRRC32* mRNA expression did not differ significantly between mutant LRRC32 (A407T)− or wild-type (WT) LRRC32−transfected $CD4^+CD25^-$ T cells of four independent healthy donors (see Supplementary Figure S3 online). However, flow cytometric analyses (FACS) showed a significant lower expression on the cell surface (Bonferroni-Holm corrected P-value = 0.044) (Figure 1) and a significant higher intracellular amount of the protein (Bonferroni-Holm corrected P-value = 0.020) in A407T-LRRC32-transfected $CD4^+CD25^-$ T cells than in WT LRRC32-transfected T cells (see Supplementary Figure S4 online). Likewise, immunofluorescence microscopy analysis in Cos-7 cells indicated lower surface expression and intracellular retention of mutated GARP (Figure 2). These observations indicate that protein production per se is not affected by the mutation, but in line with bioinformatics predictions, the folding/stabilization or posttranslational modifications necessary for the transport of GARP to the cell surface are impaired. Simultaneous measurement of additional Treg markers showed a significantly lower expression of CTLA4 ($P = 0.034$) and a tendency toward reduced FOXP3 and neuropilin expression in A407T-LRRC32-transfected $CD4^+CD25^-$ T cells, indicating an overall dampening of the Treg gene signature (see Supplementary Figures S5 and S6 online).

FACS analyses of unstimulated T-cell subtypes obtained from AD patients (n = 13) showed a significantly lower extracellular GARP expression on $CD3^+$ ($P = 0.036$), $CD4^+CD25^-$ ($P = 0.028$), and $CD4^+CD25^+$ T cells ($P = 0.035$) for A407T mutation carriers (Figure 3). After treatment of $CD4^+CD25^-$ T cells obtained from AD patients carrying the A407T variant with TGF-β, $CD25^+FOXP3^+$ T cells showed a significantly lower surface expression of GARP ($P = 0.017$) than cells from WT carriers (see Supplementary Figure S7 online).

Further, we observed a lower conversion rate of $CD4^+CD25^-$ T cells into $GARP^+FOXP3^+$ Tregs ($P = 0.004$), and a lower expression of latency-associated protein (LAP) on $GARP^+FOXP3^+$ T cells ($P = 0.026$) in carriers of A407T after stimulation with soluble GARP (see Supplementary Figure S8 online).

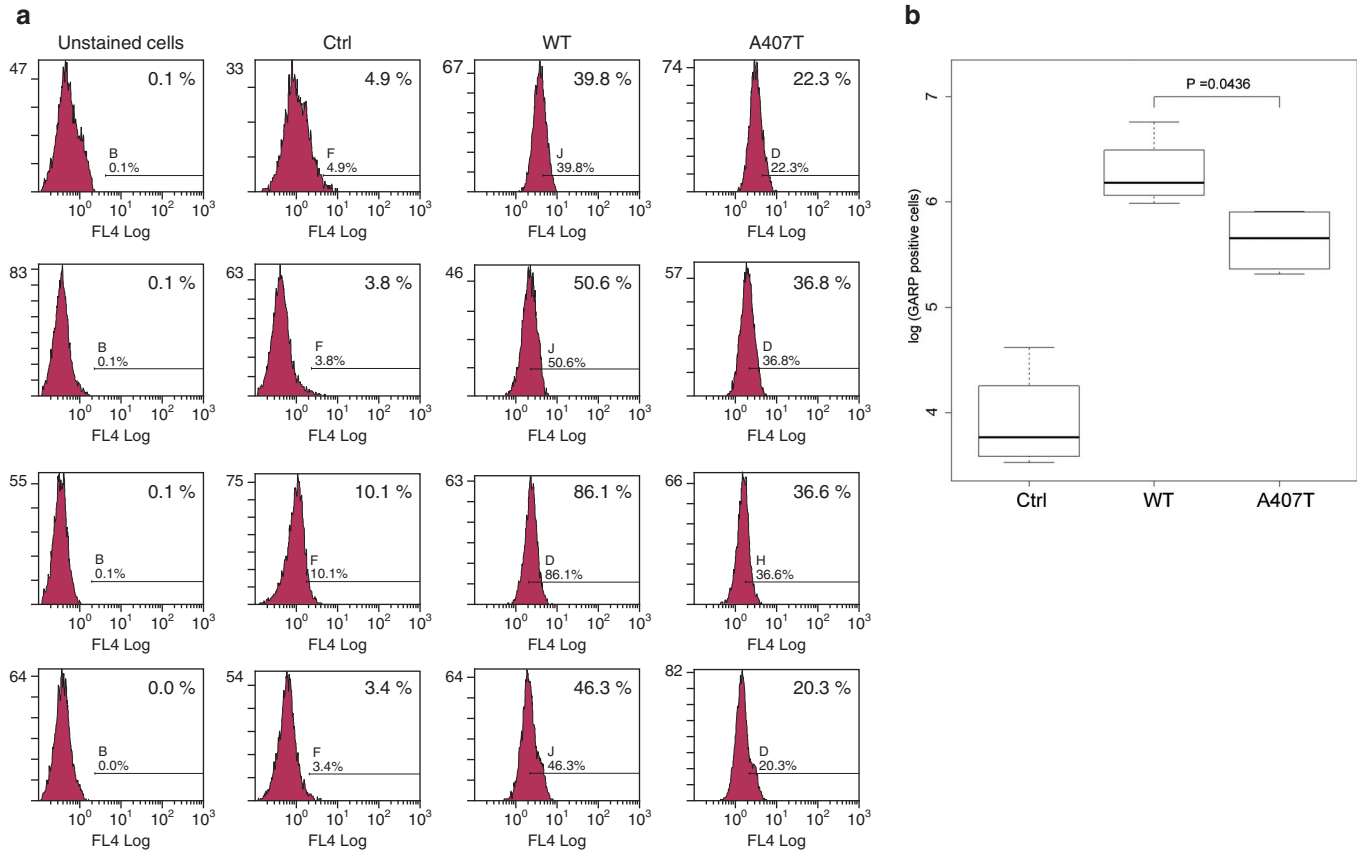

Figure 1. GARP cell surface expression on transiently transfected CD4$^+$CD25$^-$ T cells of four healthy donors. Both WT GARP or A407T GARP was overexpressed in CD4$^+$CD25$^-$ T cells, and GARP surface expression was measured by flow cytometry. Untransfected cells were used as control. (**a**) Histograms show fluorescence intensity (x-axis) versus cell number (y-axis). The values in the respective histograms indicate percentage of GARP-positive cells. (**b**) Boxplots show log-transformed data of the three groups (control, WT, A407T) normalized to the unstained cells. Ctrl, control; WT, wild type.

TGF-β is a pleiotropic cytokine, which critically shapes effector and memory T-cell populations and regulates inflammatory responses (Banchereau et al., 2012), and altered TGF-β signaling has been implicated in the pathology of many immune-mediated diseases, including AD (Frischmeyer-Guerrerio et al., 2013). TGF-β is secreted in a biologically latent form, which may bind to GARP expressed on the surface of Tregs via LAP. Upon activation through various processes, including contact with integrin-$\alpha_v\beta_6$–expressing cells, biologically active TGF-β is released from the complex of latent TGF-β and latent TGF-β–binding protein (the large latent complex) to bind to the cell-surface TGF-β1 receptor on immune cells to execute its regulatory functions (Banchereau et al., 2012). Apart from surface anchoring of latent TGF-β (Edwards et al., 2013), GARP may be directly involved in both the production and activation of TGF-β by activated Tregs (Hahn et al., 2013; Probst-Kepper et al., 2009).

Given that antibody-mediated blockade of GARP–latent TGF-β complexes and silencing of *LRRC32* through small hairpin RNA was recently shown to inhibit the immunosuppressive function of Tregs (Cuende et al., 2015; Wang et al., 2009) and that TGF-β receptor mutations strongly predispose to AD and atopy (Frischmeyer-Guerrerio et al., 2013), it is tempting to speculate that it is the disturbed interaction of latent TGF-β with GARP through which the missense mutations identified here promote risk for inflammatory barrier diseases. Further studies will have to specify the effects of *LRRC32* missense mutations on the activation of latent TGF-β and the suppressive capacity of Treg cells in the context of cutaneous inflammation.

MATERIALS AND METHODS

Additional methods are available in the Supplementary Materials online.

Study approval

This study was approved by the local ethical committee, and participants gave written informed consent in accordance with the Declaration of Helsinki.

Study population and sample selection

All AD patients and control subjects were obtained from the GENEVA study and the PopGen biorepository, respectively, described elsewhere (Paternoster et al., 2015).

For resequencing of the 11q13.5 susceptibility region, we determined the risk haplotypes for five tagging SNPs showing nominal association in our original genome-wide association study (Esparza-Gordillo et al., 2009) within this region. Carriers of these risk haplotypes were randomly drawn from the genome-wide association study subjects and weighted by the inverse haplotype frequency, leading to a set of 31 individuals enriched for low-frequency-risk haplotypes within 11q13.5.

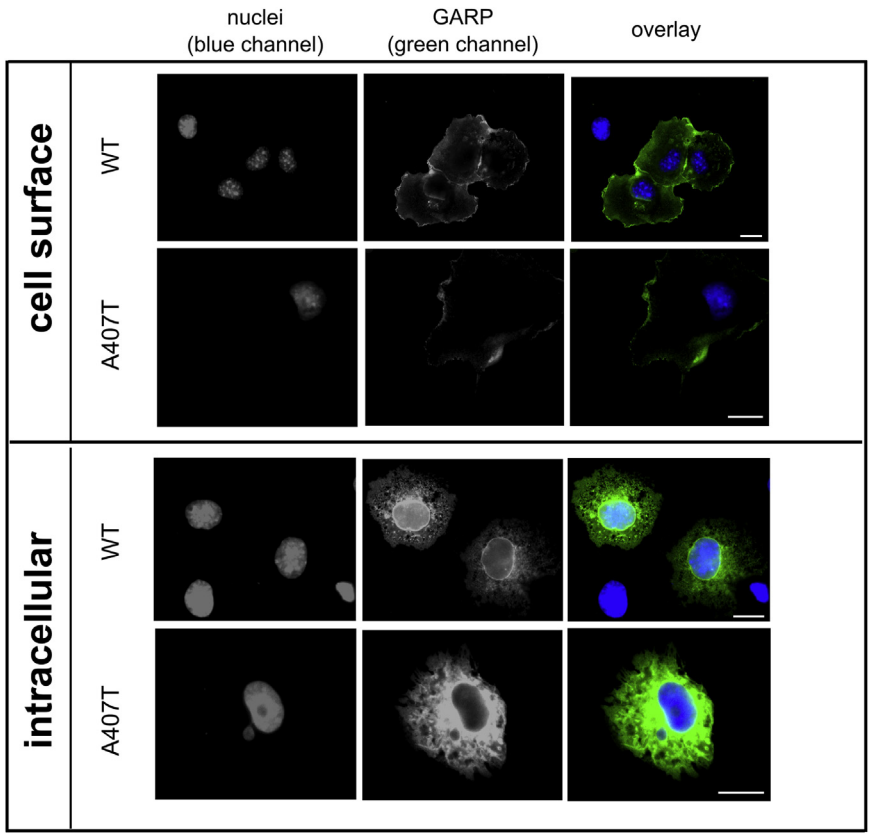

Figure 2. Cell surface and intracellular localization of GARP on transiently transfected Cos-7 cells. Cos-7 cells were transfected with either WT GARP or A407T GARP. Nuclei were stained using Hoechst 33342 dye (blue channel); GARP was stained using anti-human GARP IgG2b/goat anti-mouse Alexa-Fluor 488 (ThermoFisher Scientific, Darmstadt, Germany) antibody (green channel). The cells were imaged with a Zeiss Axiophot fluorescence microscope (Carl Zeiss, Oberkochen Germany). To visualize potential differences between WT and mutated GARP we used Cos-7 cells because of high transfection efficiency. Scale bars = 40 μm. WT, wild type.

Targeted enrichment

DNA samples were enriched for the region (11q15 chromosome 11:75,800,000–76,070,000; UCSC Genome Browser on Human Mar. 2006 (NCBI36/hg18) Assembly) using the Selector technique (Johansson et al., 2010). This technology was chosen to account for the highly repetitive nature of the region (53.05% of 11q13 is repetitive sequences), a fact that renders any hybridization-based sample enrichment approach inefficient. The Selector technology is a parallel amplification approach in a single tube. By using an intramolecular approach, targets are amplified in multiplex and do not have to be physically separated. This provides the specificity advantages of amplification without the need for dedicated instrumentation, providing a simple high-performance approach. Briefly, all DNA samples were first fragmented by restriction enzyme digestion, instead of sonication or nebulization, and then denatured. The Selector Probe library was added, and the probes were hybridized to the targeted fragments. Each Selector Probe is an oligonucleotide designed to hybridize to both ends of a targeted DNA restriction fragment, thereby guiding the targeted fragments to form circular DNA molecules. These circular molecules are then closed by ligation, a very precise reaction that ensures that only correct fragments are circularized. Only circular DNA targets are amplified, providing an enriched amplification product ready for sequencing by any next-generation procedure. By amplifying targets using specific motifs in both target fragment ends, the specificity-related reproducibility problems with hybridization-based approaches are avoided. Repeats and more complex genomic elements can be targeted with no sequencing capacity wasted on off-target regions.

Next-generation sequencing

We used SOLiD next-generation sequencing, version 3.5 (Applied Biosystems, Carlsbad, CA), mainly for its accuracy in SNV calling and high throughput. A total of 31 AD patient samples and one haplotype map (HapMap) sample as an internal positive control were indexed based on the available ABI 16X barcoding kit (Applied Biosystems, Carlsbad, CA). Instead of using SOLiD (Applied Biosystems) octant slides, we sequenced the enriched region on quads using the SOLiD 3.5 System. We multiplexed up to 11 samples per quad spot. With the barcoding strategy, we obtained an average coverage of ×795. Despite the repetitive character of the region, we were able to cover 93% on average.

Sequencing data processing and filtering

The sequence data were aligned to the reference genome (hg18) using SOLiD BioScope software (Applied Biosystems). SNV calling on the aligned data was done with BioScope and additionally with Samtools (available at http://samtools.sourceforge.net). The detected SNVs were merged sample-wise for both methods to minimize the false-negative SNV rate. The number of detected SNVs was narrowed down by filtering out all SNPs previously annotated in the public database dbSNP version 132 (National Center for Biotechnology Information, 2016) and additionally weighting the SNVs by their frequency in the 1,000 Genomes Project pilot data (minor allele frequency < 0.01) (The International Genome Sample Resource, 2016). Remaining SNVs were annotated and categorized into functional classes using our in-house tool snpActs for filtering potential functional exonic variants in terms of missense mutations. A final set of five SNVs for chromosome band 11q13.5 was carried forward to validation with Sanger sequencing.

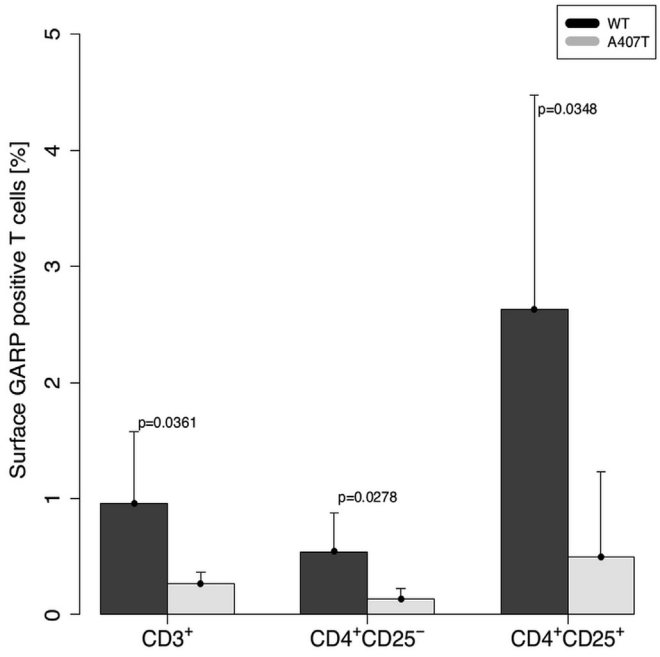

Figure 3. GARP cell surface expression on T-cell subtypes from WT GARP (n = 7) and A407T GARP (n = 6) atopic dermatitis patients. Bars indicate percentage of GARP-positive cells for pan T cells ($CD3^+$), $CD4^+CD25^-$ T cells, and $CD4^+CD25^+$ T cells. Mean values plus 95% confidence intervals and *P*-values for the different groups (WT, A407T) and cell types are presented. WT, wild type.

Genotyping

All six identified *LRRC32* missense variants were analyzed with the TaqMan allelic discrimination assays (Applied Biosystems). PCR reaction mix and PCR conditions were applied according to the manufacturer's instructions. After PCR amplification, an endpoint plate read was performed using the SDS software (Applied Biosystems).

Analysis of *LRRC32* gene expression by real-time PCR

For the analysis, 0.5 μg total RNA of 15 different tissues and cell types was reverse-transcribed using an oligo deoxythymine 18-mer ($[dT]_{18}$) primer and 25 units Superscript II (ThermoFisher Scientific, Waltham, MA) according to the manufacturer's protocol. cDNA corresponding to 10 ng total RNA served as template in a real-time PCR reaction using SYBR Premix Ex Taq II (TaKaRa Bio, Saint-Germain-en-Laye, France) and a StepOne Real Time PCR System (Applied Biosystems) as previously described (Roth et al., 2014). The following intron-spanning primers specific for *LRRC32* were used: LRRC32: 5′- ACA CCA AGA CAA AGT GCC-3′ (forward primer) and 5′- CAA GGG TCT CAG TGT CTG GC -3′ (reverse primer). Serial dilutions of cDNA were used to generate standard curves. Quantification of *LRRC32* gene expression was normalized to the housekeeping gene *RPL38* (ribosomal protein L38) using the primer pair 5′-TCA AGG ACT TCC TGC TCA CA -3′ (forward primer) and 5′-AAA GGT ATC TGC ATC GAA -3′ (reverse primer). Relative expression is given as a ratio of *LRRC32* to *RPL38* gene expression.

Transfection of $CD4^+CD25^-$ T cells

Because of their very low endogenous GARP expression and sufficient isolation yields in contrast to $CD4^+CD25^+$ T cells, the non-regulatory $CD4^+CD25^-$ fractions were transiently transfected with pIRES-GFP1 plasmids carrying either the coding sequence of human WT GARP or the human A407T GARP using an adapted diethylaminoethyl-dextran protocol as described elsewhere (Gulick, 2001). Briefly, 2×10^6 $CD4^+CD25^-$ cells were incubated with 20 μl of 10 mg/ml diethylaminoethyl-dextran (Sigma-Aldrich, Taufkirchen, Germany) solution and 2.5 μg plasmid DNA in 1 ml serum-free RPMI medium at 37 °C in a humidified atmosphere. After 4 hours of incubation, cells were washed twice with growth medium supplemented with 10% fetal calf serum (PAN Biotech, Aidenbach, Germany) followed by stimulation with 5 μg/ml phorbol myristate acetate and 10 ng/ml concanavalin A (both from Sigma-Aldrich). The cells were incubated at 37 °C for 24 hours, harvested and subjected to flow cytometric analysis. Untransfected $CD4^+CD25^-$ T cells were used as control.

LRRC32 mRNA isolation, cDNA synthesis, and reverse transcriptase-PCR

RNA from transfected $CD4^+CD25^-$ T cells (WT LRRC32 or A407T LRRC32) and untransfected $CD4^+CD25^-$ T cells was isolated using the RNeasy Mini Kit (Qiagen, Hilden, Germany) in combination with a DNase I (Qiagen, Hilden, Germany) digestion treatment. Next, 1 μg of RNA was reverse-transcribed using oligo$(dT)_{18}$ primers and the RevertAid RT Reverse Transcription Kit (ThermoFisher Scientific, Darmstadt, Germany) according to the manufacturer's protocol. End-point reverse transcriptase-PCR was performed using Pfu Turbo DNA polymerase (Agilent, Santa Clara, CA) according to the manufacturer's protocol in a RoboCycler (Stratagene, San Diego, CA) with 35 amplification cycles for *LRRC32* transcripts (used primers 5′-3′: hLRRC32_F ATGAGACCCCAGATCCTGCT; hLRRC32_R TTAGGCTTTATACTGTTGGTTAAAC) and 25 cycles for *β-actin* transcripts (used primers 5′-3′: hβ-actin_F GGATTCCT ATGTGGGCGACGAGG; hβ-actin_R CACGGAGTACTTGCGCTCA GGAGG). PCR products were visualized on a 1.5% agarose gel (containing 0.0025% Midori Green [Biozym, Hamburg, Germany]) by using a Bio Vision Gel documentation system (PeqLab, Erlangen, Germany).

Detection of GARP in transfected T cells by FACS

For detection of GARP in transfected $CD4^+CD25^-$ T cells from healthy donors, a mouse allophycocyanine-conjugated anti-human GARP antibody (BioLegend, Fell, Germany) was used for flow cytometry (FC500, Beckman Coulter, Krefeld, Germany). For intracellular staining the cells were permeabilized and fixed using Cytofix/Cytoperm solution (Becton Dickson, Franklin Lakes, NY) according to the manufacturer's protocol. Permeabilized cells were washed twice with BD Perm/Wash buffer (Becton Dickson) and stained with anti-human GARP antibody for 1 hour. For cell membrane detection of GARP, cells were directly incubated with anti-human GARP antibody after blocking and washing the cells with phosphate buffered saline (PBS) supplemented with 2 mmol/L EDTA and 0.5% BSA. After incubation, cells were subjected to flow cytometric analysis and data were analyzed with CXP Analysis software (Beckman Coulter, Brea, CA).

Detection of GARP by immunocytochemistry

Cos-7 cells were grown on glass coverslips and transiently transfected with pIRES-GFP1 plasmids carrying either the coding sequence of human WT GARP or human A407T GARP. After 48 hours of incubation in a humidified atmosphere at 37 °C and 5% CO_2, cells were fixed in 3.7% formaldehyde in PBS for 10 minutes at 37 °C and blocked with 3% BSA in PBS for 30 minutes. For intracellular staining, fixed cells were additionally permeabilized for

5 minutes using 0.5% Triton X-100 (ThermoFisher Scientific) in PBS before blocking with BSA. Fixed cells were stained with anti-human GARP IgG2b antibody (Enzo Life Sciences, Lörrach, Germany) followed by goat anti-mouse Alexa-Fluor 488 (ThermoFisher Scientific) secondary antibody. Nuclei were counterstained with Hoechst 33342 dye (1:5000 in PBS, ThermoFisher Scientific) for 2 minutes. Cells were washed with PBS after each step. Coverslips were rinsed and mounted on slides using VectaShield mounting medium (Vector Laboratories, Burlingame, CA). Images were collected on a Zeiss Axiophot fluorescence microscope (Carl Zeiss, Oberkochen, Germany) with an AxioCam MRm and analyzed by the Axio Vision release 4.8 software (Carl Zeiss).

Detection of specific T-cell markers in transfected T cells by FACS

For cytotoxic T-lymphocyte–associated protein 4 (CTLA4) staining, transfected $CD4^+CD25^-$ T cells from healthy donors were incubated with a phycoerythrin-conjugated anti-CTLA4 (anti-CD152) antibody (Miltenyi Biotec, Teterow, Germany). For staining of neuropilin, an allophycocyanine-conjugated anti-neuropilin antibody (Miltenyi Biotec) was used. Cells were directly incubated with appropriate antibodies (1 hour) after blocking and washing the cells with PBS supplemented with 2mmol/L EDTA and 0.5% BSA. Intracellular staining of FOXP3 was performed using a phycoerythrin-conjugated anti-FOXP3 antibody (eBioscience, San Diego, CA). Before staining, cells were permeabilized, fixed, and washed according to the Cytofix/Cytoperm protocol (Becton Dickson, Franklin Lakes, NY).

Detection of GARP and specific T-cell markers in T cells of AD patients by FACS

Expression of GARP on unstimulated T-cell subtypes of 13 AD patients (WT, n = 7; A407T, n = 6) was measured directly after isolation. The following monoclonal antibodies were used for costaining: unconjugated anti-GARP (clone 7B11) (Biolegend, Fell, Germany); anti-CD3-PE Cy 5 (clone UCHT1) and anti-CD4-APC (clone RPAT4) (both from BD Biosciences Pharmingen, Heidelberg, Germany); and anti-CD25-PE (clone 4E3) (Miltenyi Biotec).

For all other measurements, $CD4^+CD25^-$ T cells were stimulated with 100 U/ml recombinant human IL-2 (PeproTech, Rocky Hill, NJ), 2 μg/ml anti-CD28 (clone 37407), and 5 ng/ml recombinant human TGF-β or 10 μg/ml soluble GARP (#6055-LR, R&D Systems, Wiesbaden, Germany) at 1×10^6 cells/ml on 5 μg/ml anti-CD3 (clone UCHT1)–coated plates for 3 days (all from R&D Systems). Expression of GARP, LAP, FOXP3, and CD25 after TGF-β or soluble GARP stimulation was measured on day 3 of culture by flow cytometry. Condition without soluble GARP or stimulation was used as control. The following monoclonal antibodies were used: anti-GARP-APC (clone 7B11) and CD25-fluorescein isothiocyanate (clone M-A251) (both from BD Biosciences Pharmingen) and LAP-PE (clone FNLAP), FOXP3-FITC (clone 236A/E7), and FOXP3-PE (clone PCH101) (all from eBioscience, San Diego, CA).

Stained cells were acquired on a FACSCanto (BD Biosciences Pharmingen). Data were analyzed with FACSDiva software (BD Biosciences Pharmingen).

Statistics

Association testing of validated variants with AD was carried out by the gene-based cumulative minor allele test (Zawistowski et al., 2010), which jointly analyses a set of variants within the same gene followed by logistic regression for each single variant separately adjusted for sex.

GARP expression FACS data were first log-transformed and three groups (control, WT LRRC32, and mutant LRRC32 [A407T]) were compared by analysis after a Bonferroni-Holm –corrected post hoc analysis. For specific T-cell marker expression (CTLA4, FOXP3, neuropilin), *P*-values were calculated using the one-sample *t* test on log-transformed expression ratios (A407T/WT LRRC32).

For comparing GARP and specific T-cell marker expression in T cells between WT and A407T AD patients *P*-values were calculated using the Welch test on positive cell counts. All statistical analyses were carried out using R, version 3.2.4. (R Development Core Team, 2008).

CONFLICT OF INTEREST

The authors state no conflict of interest.

ACKNOWLEDGMENTS

We thank all patients, their families, and healthy control individuals for their contributions. This work was supported by grants (WE2678/6-1, WE2678/6-2, WE2678/9) from the German Research Foundation ande:Med sysINFLAME grant no. 01ZX1306A from the German Federal Ministry of Education and Research. The funders had no role in study design, data collection and analysis, decision to publish, or preparation of the manuscript.

SUPPLEMENTARY MATERIAL

Supplementary material is linked to the online version of the paper at www.jidonline.org, and at http://dx.doi.org/10.1016/j.jid.2016.07.009.

REFERENCES

Anderson CA, Boucher G, Lees CW, Franke A, D'Amato M, Taylor KD, et al. Meta-analysis identifies 29 additional ulcerative colitis risk loci, increasing the number of confirmed associations to 47. Nat Genet 2011;43:246–52.

Banchereau J, Pascual V, O'Garra A. From IL-2 to IL-37: the expanding spectrum of anti-inflammatory cytokines. Nat Immunol 2012;13:925–31.

Barrett JC, Hansoul S, Nicolae DL, Cho JH, Duerr RH, Rioux JD, et al. Genome-wide association defines more than 30 distinct susceptibility loci for Crohn's disease. Nat Genet 2008;40:955–62.

Betz RC, Petukhova L, Ripke S, Huang H, Menelaou A, Redler S, et al. Genome-wide meta-analysis in alopecia areata resolves HLA associations and reveals two new susceptibility loci. Nat Commun 2015;6:5966.

Bonnelykke K, Matheson MC, Pers TH, Granell R, Strachan DP, Alves AC, et al. Meta-analysis of genome-wide association studies identifies ten loci influencing allergic sensitization. Nat Genet 2013;45:902–6.

Chen R, Jiang X, Sun D, Han G, Wang F, Ye M, et al. Glycoproteomics analysis of human liver tissue by combination of multiple enzyme digestion and hydrazide chemistry. J Proteome Res 2009;8:651–61.

Cuende J, Lienart S, Dedobbeleer O, van der Woning B, De Boeck G, Stockis J, et al. Monoclonal antibodies against GARP/TGF-beta1 complexes inhibit the immunosuppressive activity of human regulatory T cells in vivo. Sci Transl Med 2015;7:284ra56.

Edwards JP, Fujii H, Zhou AX, Creemers J, Unutmaz D, Shevach EM. Regulation of the expression of GARP/latent TGF-beta1 complexes on mouse T cells and their role in regulatory T cell and Th17 differentiation. J Immunol 2013;190:5506–15.

Ellinghaus D, Baurecht H, Esparza-Gordillo J, Rodriguez E, Matanovic A, Marenholz I, et al. High-density genotyping study identifies four new susceptibility loci for atopic dermatitis. Nat Genet 2013;45:808–12.

Esparza-Gordillo J, Weidinger S, Folster-Holst R, Bauerfeind A, Ruschendorf F, Patone G, et al. A common variant on chromosome 11q13 is associated with atopic dermatitis. Nat Genet 2009;41:596–601.

Ezell SA, Polytarchou C, Hatziapostolou M, Guo A, Sanidas I, Bihani T, et al. The protein kinase Akt1 regulates the interferon response through phosphorylation of the transcriptional repressor EMSY. Proc Natl Acad Sci USA 2012;109:E613–21.

Ferreira MA, Matheson MC, Duffy DL, Marks GB, Hui J, Le Souef P, et al. Identification of IL6R and chromosome 11q13.5 as risk loci for asthma. Lancet 2011;378:1006–14.

Franke A, McGovern DP, Barrett JC, Wang K, Radford-Smith GL, Ahmad T, et al. Genome-wide meta-analysis increases to 71 the number of confirmed Crohn's disease susceptibility loci. Nat Genet 2010;42:1118–25.

Frischmeyer-Guerrerio PA, Guerrerio AL, Oswald G, Chichester K, Myers L, Halushka MK, et al. TGFbeta receptor mutations impose a strong predisposition for human allergic disease. Sci Transl Med 2013;5:195ra94.

Garapaty S, Xu CF, Trojer P, Mahajan MA, Neubert TA, Samuels HH. Identification and characterization of a novel nuclear protein complex involved in nuclear hormone receptor-mediated gene regulation. J Biol Chem 2009;284:7542–52.

Gulick T. Transfection using DEAE-dextran. Curr Protoc Mol Biol 2001; Chapter 9:Unit 9.2.

Hahn SA, Stahl HF, Becker C, Correll A, Schneider FJ, Tuettenberg A, et al. Soluble GARP has potent antiinflammatory and immunomodulatory impact on human CD4(+) T cells. Blood 2013;122:1182–91.

The International Genome Sample Resource. ISGR: The International Genome Sample Resource, http://www.1000genomes.org/; 2016 (accessed 28 July 2016).

Johansson H, Isaksson M, Sorqvist EF, Roos F, Stenberg J, Sjoblom T, et al. Targeted resequencing of candidate genes using selector probes. Nucleic Acids Res 2010;39:e8.

Kottyan LC, Davis BP, Sherrill JD, Liu K, Rochman M, Kaufman K, et al. Genome-wide association analysis of eosinophilic esophagitis provides insight into the tissue specificity of this allergic disease. Nat Genet 2014;46:895–900.

Krawczak M, Nikolaus S, von Eberstein H, Croucher PJ, El Mokhtari NE, Schreiber S. PopGen: population-based recruitment of patients and controls for the analysis of complex genotype-phenotype relationships. Community Genet 2006;9:55–61.

National Center for Biotechnology Information. dbSNP Short Genetic Variations, http://www.ncbi.nlm.nih.gov/SNP/; 2016 (accessed 28 July 2016).

Paternoster L, Standl M, Chen CM, Ramasamy A, Bonnelykke K, Duijts L, et al. Meta-analysis of genome-wide association studies identifies three new risk loci for atopic dermatitis. Nat Genet 2012;44:187–92.

Paternoster L, Standl M, Waage J, Baurecht H, Hotze M, Strachan DP, et al. Multi-ancestry genome-wide association study of 21,000 cases and 95,000 controls identifies new risk loci for atopic dermatitis. Nat Genet 2015;47:1449–56.

Probst-Kepper M, Geffers R, Kroger A, Viegas N, Erck C, Hecht HJ, et al. GARP: a key receptor controlling FOXP3 in human regulatory T cells. J Cell Mol Med 2009;13:3343–57.

R Development Core Team. R: A language and environment for statistical computing. Vienna, Austria: R Foundation for Statistical Computing, http://www.R-project.org; 2008 (accessed 28 July 2016).

Ramasamy A, Curjuric I, Coin LJ, Kumar A, McArdle WL, Imboden M, et al. A genome-wide meta-analysis of genetic variants associated with allergic rhinitis and grass sensitization and their interaction with birth order. J Allergy Clin Immunol 2011;128:996–1005.

Roth SA, Simanski M, Rademacher F, Schroder L, Harder J. The pattern recognition receptor NOD2 mediates *Staphylococcus aureus*-induced IL-17C expression in keratinocytes. J Invest Dermatol 2014;134:374–80.

Tran DQ, Andersson J, Wang R, Ramsey H, Unutmaz D, Shevach EM. GARP (LRRC32) is essential for the surface expression of latent TGF-beta on platelets and activated FOXP3+ regulatory T cells. Proc Natl Acad Sci USA 2009;106:13445–50.

Wang R, Kozhaya L, Mercer F, Khaitan A, Fujii H, Unutmaz D. Expression of GARP selectively identifies activated human FOXP3+ regulatory T cells. Proc Natl Acad Sci USA 2009;106:13439–44.

Wang R, Zhu J, Dong X, Shi M, Lu C, Springer TA. GARP regulates the bioavailability and activation of TGFbeta. Mol Biol Cell 2012;23:1129–39.

Weidinger S, Novak N. Atopic dermatitis. Lancet 2016;387:1109–22.

Weidinger S, Willis-Owen SA, Kamatani Y, Baurecht H, Morar N, Liang L, et al. A genome-wide association study of atopic dermatitis identifies loci with overlapping effects on asthma and psoriasis. Hum Mol Genet 2013;22:4841–56.

Zawistowski M, Gopalakrishnan S, Ding J, Li Y, Grimm S, Zollner S. Extending rare-variant testing strategies: analysis of noncoding sequence and imputed genotypes. Am J Hum Genet 2010;87:604–17.